ELSEVIER

Atmospheric Research 34 (1994) 299–308

ATMOSPHERIC RESEARCH

On the limitation of using asymmetry factor for radiative transfer involving cirrus clouds

Qiang Fu, Y. Takano

Department of Meteorology/CARSS, University of Utah, Salt Lake City, UT 84112, USA

(Received January 12, 1992; revised version accepted June 4, 1993)

Abstract

We investigate the limitation of using the asymmetry factor through the Henyey–Greenstein function in representing the scattering phase function for radiative transfer in ice clouds containing hexagonal ice crystals. Relative accuracy checks for solar fluxes are carried out using three cirrus cloud size distributions. The flux results computed from the Henyey–Greenstein phase function, based on the asymmetry factor, differ significantly from those computed from the phase function for hexagonal ice crystals. For optically thin ice clouds, the relative error can be as large as 70%. The maximum absolute error in solar reflected fluxes is 27 Wm^{-2}. The present flux calculations demonstrate that the phase functions for ice crystals which contain strong forward scattering peak and specific halos and back scattering features cannot be adequately represented by a single parameterization in terms of the asymmetry factor.

1. Introduction

The scattering phase function of cloud and aerosol particles is highly anisotropic and depends on the particle shape and size distribution. For radiative transfer calculations, it is often convenient to approximate the actual scattering phase function with the Henyey–Greenstein function which is based on a single parameter, the asymmetry factor (see, e.g., van de Hulst and Irvine, 1963; Stephens, 1984; Wiscombe et al., 1984; Ackerman et al., 1988; Liou et al., 1988; Tsay et al., 1989). For water clouds and aerosol particles, as demonstrated by Hansen (1969), this approximation leads to errors of less than 1% in the computations of fluxes. This error is comparable to other approximations such as the neglect of polarization (Hansen, 1971). In Hansen's (1969) computations, the actual phase functions of cloud/aerosol particles were obtained by using the Mie

0169-8095/94/$07.00
SSDI 0169-8095(93)E0112-C

scattering theory, which assumes that the particles are spherical. The simple representation of the scattering phase function using the asymmetry factor can greatly simplify the parameterization for single-scattering properties of cloud/aerosol particles.

High-level cirrus clouds consist almost exclusively of nonspherical ice crystals of various shapes such as bullet rosettes, plates and columns. Because of the hexagonal structure of ice crystals, the Mie scattering theory cannot simulate the radiative properties of cirrus clouds (Kinne and Liou, 1989; Takano and Liou, 1989a). The question is then raised, is the asymmetry factor through Henyey–Greenstein function adequate to approximate the scattering phase function of ice clouds in the flux calculations? This note will address this question. In the next section, we present the single-scattering properties of hexagonal ice crystals and the Henyey–Greenstein function. The numerical procedure to compute the solar albedo is given in Section 3. Computational results and conclusions are given in Section 4.

2. Single-scattering property calculations

The single-scattering properties, including the extinction coefficient, single-scattering albedo and phase function, are computed from the geometric ray tracing program developed by Takano and Liou (1989a). The hexagonal ice crystals are assumed to be randomly oriented in space. In view of the observed ice crystal sizes in cirrus clouds ($\sim$20–2000 μm), the ray tracing method should be valid for solar wavelengths (0.2–4 μm). Based on observations by Ono (1969) and Auer and Veal (1970), the aspect ratio, L(length)/D(diameter), of the ice crystals may be related to the crystal length L. Then the ice crystal size distribution can be denoted by $n(L)$. In the present study, three ice crystal size distributions are employed. The first two are for the cirrostratus (Cs) and cirrus uncinus (Ci uncinus) presented by Heymsfield (1975), while the third one is Ci (1 November), which was collected during the 1986 FIRE cirrus experiments (A. Heymsfield, pers. commun.). These size distributions are displayed in Fig. 1. For scattering and absorption calculations, these size distributions have been discretized in five regions. The aspect ratios, L/D, used are 20/20, 50/40, 120/60, 300/100 and 750/160 in units of μm/μm, roughly corresponding to the observations reported by Ono (1969) and Auer and Veal (1970). The refractive indices for ice compiled by Warren (1984) are used in the scattering calculations.

Table 1 shows the extinction coefficient, single-scattering albedo and asymmetry factor for the three ice cloud models in six solar spectral intervals. The optical depth for cirrus clouds is given by βz, where β is the extinction coefficient and z is the cloud thickness. The asymmetry factor is defined as

$$g=\tfrac{1}{2}\int_{-1}^{1} P(\cos\theta)\cos\theta \mathrm{d}(\cos\theta), \tag{1}$$

where $P(\cos\theta)$ is the scattering phase function and θ denotes the scattering angle.

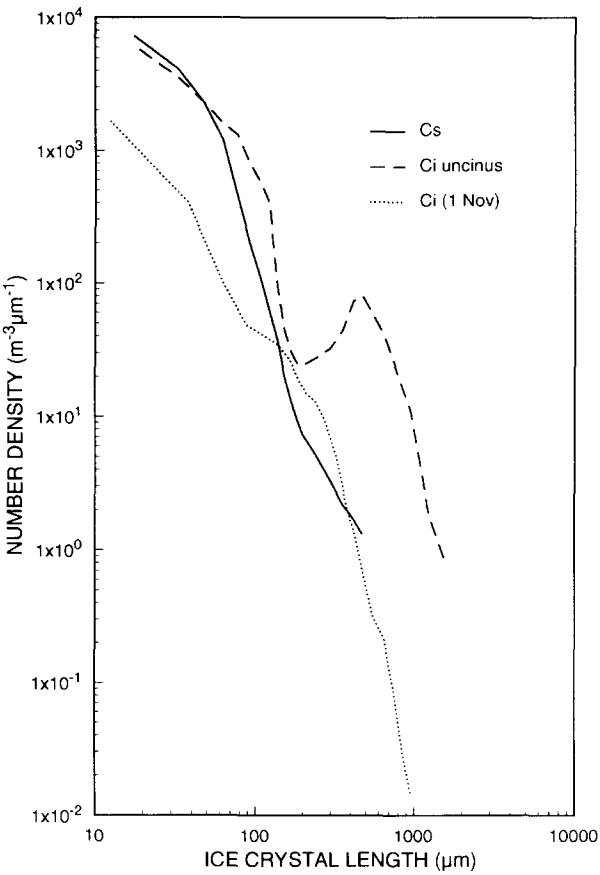

Fig. 1. The observed ice crystal size distributions for Cs (——), Ci uncinus (– –), and Ci (1 Nov) (···).

Table 1 illustrates that the asymmetry factor, g, generally increases with increasing particle size. Using the asymmetry factor, g, the Henyey–Greenstein function is defined by

$$P_{\mathrm{H-G}}(\cos\theta)=\frac{1-g^2}{(1+g^2-2g\cos\theta)^{3/2}}. \tag{2}$$

The analytic phase function has been used extensively in the literature and its merits have been discussed by van de Hulst and Grossman (1968). The Henyey–Greenstein phase function can be expanded in terms of Legendre polynomials, P_l, in the form

$$P_{\mathrm{H-G}}(\cos\theta)=\sum_{l=0}^{\infty}(2l+1)g^l P_l(\cos\theta). \tag{3}$$

Table 1
Extinction coefficient $\beta(km^{-1})$, single-scattering albedo $\tilde{\omega}$ and asymmetry factor, g, for the three cirrus models in six solar spectral intervals

Spectral region (μm)	Cloud type*	β (km^{-1})	$\tilde{\omega}$	g
0.20–0.69	Cs	0.3865	1.0000	0.7824
	Ci uncinus	2.6058	1.0000	0.8404
	Ci (1 Nov)	0.2021	1.0000	0.8154
0.69–1.30	Cs	0.3865	0.9995	0.7905
	Ci uncinus	2.6058	0.9981	0.8448
	Ci (1 Nov)	0.2021	0.9989	0.8195
1.30–1.90	Cs	0.3865	0.9658	0.8100
	Ci uncinus	2.6058	0.9004	0.8778
	Ci (1 Nov)	0.2021	0.9365	0.8473
1.90–2.50	Cs	0.3865	0.9185	0.8436
	Ci uncinus	2.6058	0.7996	0.9116
	Ci (1 Nov)	0.2021	0.8603	0.8821
2.50–3.50	Cs	0.3865	0.5321	0.9653
	Ci uncinus	2.6058	0.5309	0.9728
	Ci (1 Nov)	0.2021	0.5311	0.9626
3.50–4.00	Cs	0.3865	0.7117	0.8593
	Ci uncinus	2.6058	0.5889	0.9356
	Ci (1 Nov)	0.2021	0.6326	0.9137

*The ice water contents for Cs, Ci uncinus and Ci (1 Nov) are 4.765×10^{-3}, 1.116×10^{-1} and $4.968\times10^{-3}\,gm^{-3}$, respectively. The corresponding mean effective sizes are 41.5, 123.6 and 75.1 μm. The mean effective size is defined by $\int D\cdot DLn(L)/\int DLn(L)dL$, where D and L are the diameter and length of a hexagonal ice crystal, respectively, and $n(L)$ denotes the ice crystal size distribution.

The phase functions computed from the geometric ray tracing program at the 0.55 μm wavelength for cirrostratus and cirrus uncinus are shown in Fig. 2a and b, respectively. The 22° and 46° halos produced by two refracted rays are well illustrated in the diagram, as is the forward diffraction peak. The maximum occurring between 150° and 160° is produced by rays undergoing two internal reflections. At $\theta=0°$, the phase-function value is infinity (∞) due to the δ-function transmission through parallel planes of ice crystals (Takano and Liou, 1989a). The contribution from the δ-function transmission with respect to the entire scattered light, f_δ, is 0.126 and 0.155 for Cs and Ci uncinus, respectively. The exact phase functions shown in Fig. 2 are a little different from those shown in Fig. 3 of Takano and Liou (1989a). The latter has not incorporated the contribution of the δ-function transmission. The phase function with δ-forward peak, $P(\cos\theta)$, can be related to the phase function without δ-forward peak, $P'(\cos\theta)$, by,

$$P(\cos\theta)=2f_\delta\delta(\cos\theta-1)+(1-f_\delta)P'(\cos\theta), \tag{4}$$

where δ is the δ-function. Also shown in Fig. 2 are the Henyey–Greenstein phase functions using the asymmetry factor, g, of 0.7824 for Cs and 0.8404 for Ci uncinus at 0.55 μm. For the Ci (1 Nov), the phase function is between those for Cs and Ci uncinus and is not presented here. In the next sections, using broadband

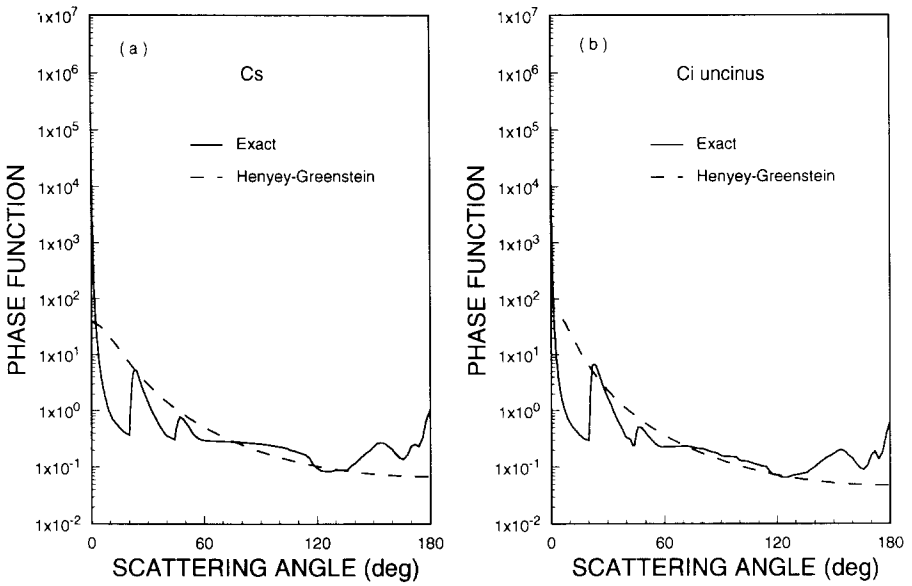

Fig. 2. Phase functions for scattering by (a) Cs and (b) Ci uncinus at 0.55 μm. The exact phase functions are from the geometric ray-tracing program, and Henyey–Greenstein functions are obtained with g=0.7824 for Cs and g=0.8404 for Ci uncinus.

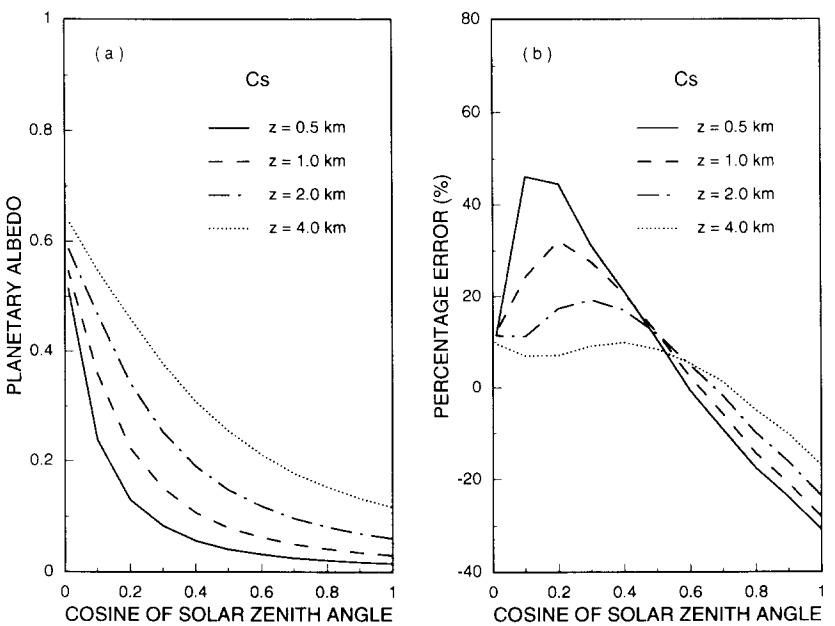

Fig. 3. (a) Planetary albedo computed from the doubling method using the exact phase function for Cs as a function of the cosine of the solar zenith angle and cloud thickness and (b) the corresponding percentage error due to the doubling method using analytic Henyey–Greenstein phase function.

planetary albedo we will demonstrate that a simple representation of the phase function using the asymmetry factor for the transfer of solar radiation in ice clouds is inadequate.

3. Numerical procedure

The planetary albedo, which is the ratio of the solar radiation reflected from a plane parallel atmosphere to the incident radiation, is expressed as

$$r_i(\mu_0)=\frac{1}{\pi}\int_0^{2\pi}\int_0^1 R_i(\mu,\mu_0,\phi-\phi_0)\,\mu\,\mathrm{d}\mu\,\mathrm{d}\phi, \tag{5}$$

where μ and ϕ are the cosine of the zenith angle and the azimuthal angle, respectively, for an outgoing light beam; μ_0 is the cosine of the solar zenith angle, ϕ_0 is the corresponding azimuthal angle; $R_i(\mu, \mu_0, \phi-\phi_0)$ is the reflection function, which gives the angular distribution of the scattered light in the upper hemisphere; i is the index of the band in the solar spectrum. The broadband planetary albedo is then given by

$$r(\mu_0)=\sum_{i=1}^{6} r_i(\mu_0)a_i. \tag{6}$$

where a_i is the fraction of solar energy contained in the individual bands.

$R_i(\mu, \mu_0, \phi-\phi_0)$ is computed from the doubling principle developed in Takano and Liou (1989b). We start the doubling process with an optical depth of 10^{-6}. The Henyey–Greenstein functions are expanded in the Legendre polynomial series with 150 terms, while the scattering phase functions computed from geometric optics are expanded with 250 terms. The higher number of Legendre expansion is required for the latter to resolve salient features such as halos. To optimize the computational effort, the forward peak of the phase function $P'(\cos\theta)$ which is computed from geometric optics is truncated as described in Takano and Liou (1989b). Then, the truncated fraction and the contribution of the δ-transmission part have been accounted for by using the similarity principle (Takano and Liou, 1989b). The forward diffraction peak of the Henyey–Greenstein function is also truncated when the asymmetry factor exceeds 0.9. The relative error in the present doubling calculation is less than $\sim 0.1\%$.

4. Computational results and conclusions

Figs. 3a–5a show the broadband planetary solar albedo of Cs, Ci uncinus, and Ci (1 Nov), respectively, by using the scattering phase function computed from geometric optics, as a function of the cosine of the solar zenith angle and cloud thickness. The results in Figs. 3a–5a provide a reference in a relative sense. Figs.

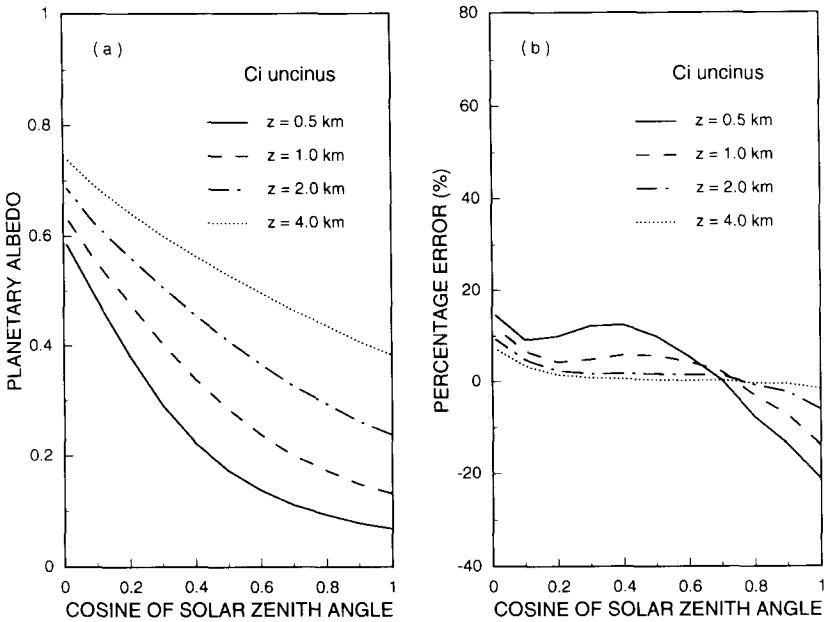

Fig. 4. Same as Fig. 2, except for Ci uncinus.

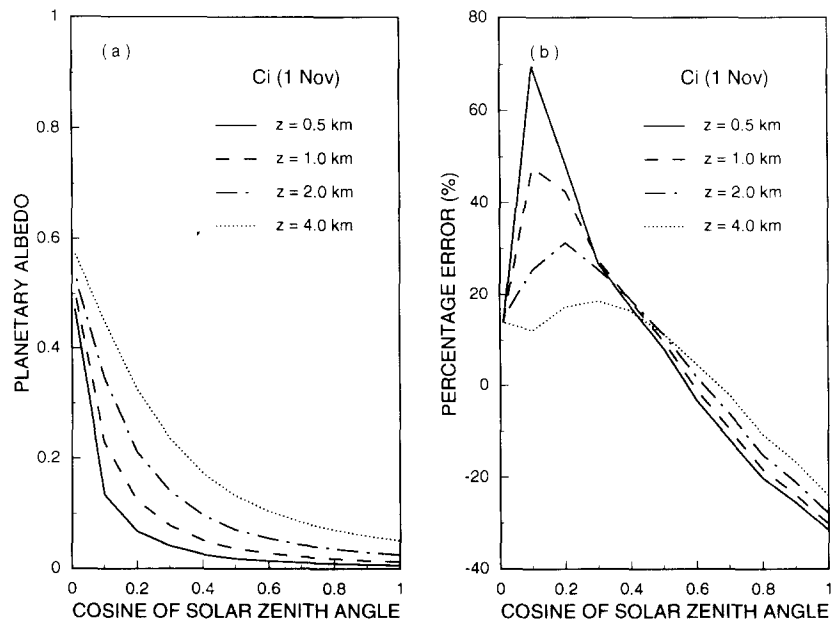

Fig. 5. Same as Fig. 2, except for Ci (1 Nov).

3b–5b show the corresponding percentage error of the doubling method with the analytic Henyey–Greenstein phase function. The Henyey–Greenstein phase function, based on the asymmetry factor, yields planetary albedos very different from those obtained with the scattering phase function from the geometric ray tracing program. This is especially true for optically thin ice clouds where the single-scattering process is important. An error as large as 70% occurs for $z=0.5$ km and $\mu_0=0.1$ in the case of Ci (1 Nov). The percentage errors in planetary albedos for each cloud type reduce significantly as the cloud thickness increases. This is because the multiple scattering process, which is more important for thicker clouds due to the larger optical depths, at least partially averages out the details of the phase function. By comparing the results in Fig. 3b with those in Fig. 5b, we find that the percentage errors for Cs with $z=0.5$, 1 and 2 km are almost the same as those for Ci (1 Nov) with $z=1$, 2 and 4 km, respectively. This is because the extinction coefficient of Cs is about twice as large as that of Ci (1 Nov). The difference in percentage errors between Ci uncinus and other two can also be interpreted in terms of the optical depth. It can be concluded that the relative error produced by the Henyey–Greenstein phase function is a function of optical depth and solar zenith angle. In the cases of Cs and Ci (1 Nov), the percentage errors are $\sim 10\%$ for a μ_0 of 0.5. From Figs. 3b–5b, it is noted that the errors change their sign from positive to negative for a μ_0 between 0.6 and 0.7. The dependence of errors on μ_0 in Figs. 3b–5b is due to deficiencies in the Henyey–Greenstein function. The Henyey–Greenstein phase function cannot reproduce scattering features of hexagonal ice crystals, such as the strong forward peak, 22° and 46° halo maxima and back scattering maxima. As shown in Fig. 2, the Henyey–Greenstein function is smaller than the exact phase function when the scattering angle is larger than $\sim 70°$. When the scattering angle is smaller than $\sim 70°$, the Henyey–Greenstein is larger than the exact except for the forward and 22° halo peaks. This pattern explains why the error is negative for small solar zenith angles and positive for the large ones. The dependence of errors on the solar zenith angle is reduced with an increase in optical depth due to multiple-scattering effect, as discussed before. Figs. 3–5 demonstrate that the analytic phase function cannot, in general, accurately simulate the transfer of solar radiation in cirrus clouds.

Fig. 6 shows errors in reflected solar fluxes produced by the doubling method using analytic Henyey–Greenstein phase function for Cs. The absolute error is obtained by multiplying the percentage error in Fig. 3b by $r(\mu_0)\mu_0 S_0$. Here $r(\mu_0)$ is the planetary albedo from Fig. 3a and S_0 is the solar constant, ~ 1360 Wm^{-2}. The maximum error in solar reflected fluxes is ~ 27 Wm^{-2}. Assuming a 20% cloud cover, the error in outgoing solar fluxes can be as large as 5 Wm^{-2}. This error is significant in climate and remote sensing studies.

The errors shown in Figs. 3b–5b can affect the simulated diurnal and annual distributions of solar energy. For example, for a latitude of 45°, the cosine of the solar zenith angle at solar noon is 0.37, 0.71 and 0.93 for winter solstice, vernal/autumnal equinox and summer solstice, respectively. Therefore, the Henyey–Greenstein phase function cools the Earth-atmospheric system all day due to a

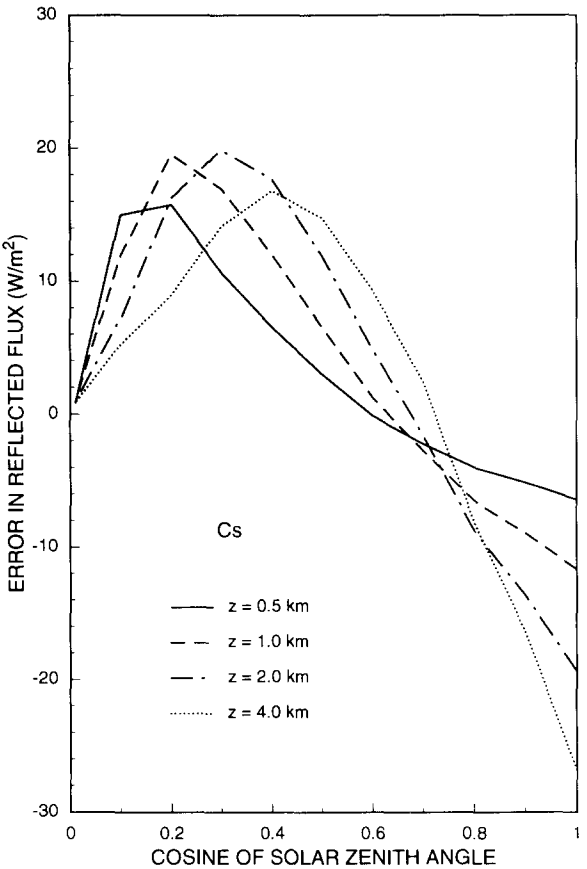

Fig. 6. Errors in reflected solar fluxes produced by the doubling method using analytic Henyey–Greenstein phase function for Cs.

larger albedo in wintertime, while in summertime, it warms the system at noon but cools it in the morning and afternoon. Therefore, the use of the simple representation of the phase function in numerical models would significantly modify the pattern of atmospheric motions.

The significance of this note is emphasized for the parameterization of radiative properties of cirrus clouds (Fu and Liou, 1993). As demonstrated by Liou et al. (1988), the δ-four-stream approximation is well suited to radiative transfer parameterizations involving flux and heating-rate calculations in aerosol and cloudy atmospheres. The expansion coefficients, $\tilde{\omega}_l$ ($l=1, 2, 3, 4$) of the scattering phase function are required in this approximation. Based on numerical computations, we find that the δ-four-stream scheme using $\tilde{\omega}_l$ from geometric optics can achieve an accuracy within $\sim 5\%$, while the δ-four-stream scheme using $\tilde{\omega}_l = (2l+1)g^l$ can produce errors as large as 50%. This again demonstrates that

a single parameter, asymmetry factor, is not sufficient to yield adequate results for radiative transfer involving cirrus clouds.

Acknowledgements

The authors would like to thank Dr. S. Kinne for his comments on the manuscript. The research work contained herein has been supported by AFOSR Grant 91-0039, NASA Grant NAG5-1050 and NSF Grant 90-24217.

References

Ackerman, T.P., Liou, K.N., Valero, F.P.J. and Pfister, L., 1988. Heating rates in tropical anvils. J. Atmos. Sci., 45: 1606–1623.

Auer, A.H., Jr. and Veal, D.L., 1970. The dimension of ice crystals in natural clouds. J. Atmos. Sci., 27: 919–926.

Fu, Q. and Liou, K.N., 1993. Parameterization of the radiative properties of cirrus clouds. J. Atmos. Sci., 50: 2008–2025.

Hansen, J.E., 1969. Exact and approximate solutions for multiple scattering by cloudy and hazy planetary atmospheres. J. Atmos. Sci., 26: 478–487.

Hansen, J.E., 1971. Multiple scattering of polarized light in planetary atmospheres. Part II: Sunlight reflected by terrestrial water clouds. J. Atmos. Sci., 28: 1400–1426.

Heymsfield, A.J., 1975. Cirrus uncinus generating cells and the evolution of cirriform clouds. J. Atmos. Sci., 32: 799–808.

Kinne, S. and Liou, K.N., 1989. The effects of the nonsphericity and size distribution of ice crystals on the radiative properties of cirrus clouds. Atmos. Res., 24: 273–284.

Liou, K.N., Fu, Q. and Ackerman, T.P., 1988. A simple formulation of the deltafour-stream approximation for radiative transfer parameterizations. J. Atmos. Sci., 45: 1940–1947.

Ono, A., 1969. The shape and riming properties of ice crystals in natural clouds. J. Atmos. Sci., 26: 138–147.

Stephens, G.L., 1984. The parameterization of radiation for numerical weather prediction and climate models. Mon. Weather Rev., 112: 826–867.

Takano, Y., and Liou, K.N., 1989a. Solar radiative transfer in cirrus clouds. Part I: Single-scattering and optical properties of hexagonal ice crystals. J. Atmos. Sci., 46: 3–19.

Takano, Y. and Liou, K.N., 1989b. Solar radiative transfer in cirrus clouds. Part II: Theory and computation of multiple scattering in an anisotropic medium. J. Atmos. Sci., 46: 20–36.

Tsay, S.-C., Stamnes, K. and Jayaweera, K., 1989. Radiative energy budget in the cloudy and hazy arctic. J. Atmos. Sci., 46: 1002–1018.

van de Hulst, H.C. and Irvine, W.M., 1963. General report on radiation transfer in planets: Scattering in model planetary atmospheres. Mem. Soc. R. Sci. Liege, 7: 78–98.

van de Hulst, H.C. and Grossman, K., 1968. Multiple light scattering in planetary atmospheres. In: The Atmospheres of Venus and Mars. Gordon and Breach, New York, 288 pp.

Warren, S.G., 1984. Optical constants of ice from ultraviolet to the microwave. Appl. Opt., 23: 1206–1225.

Wiscombe, W.J., Welch, R.M. and Hall, W.D., 1984. The effects of very large drops on cloud absorption. Part I: Parcel models. J. Atmos. Sci., 41: 1336–1355.